Research Article

Molecular Cancer Therapeutics

ARQ 197, a Novel and Selective Inhibitor of the Human c-Met Receptor Tyrosine Kinase with Antitumor Activity

Neru Munshi[2], Sébastien Jeay[1], Youzhi Li[2], Chang-Rung Chen[1], Dennis S. France[1], Mark A. Ashwell[1], Jason Hill[1], Magdi M. Moussa[1], David S. Leggett[2], and Chiang J. Li[2]

Abstract

The *met* proto-oncogene is functionally linked with tumorigenesis and metastatic progression. Validation of the receptor tyrosine kinase c-Met as a selective anticancer target has awaited the emergence of selective c-Met inhibitors. Herein, we report ARQ 197 as the first non-ATP–competitive small molecule that selectively targets the c-Met receptor tyrosine kinase. Exposure to ARQ 197 resulted in the inhibition of proliferation of c-Met–expressing cancer cell lines as well as the induction of caspase-dependent apoptosis in cell lines with constitutive c-Met activity. These cellular responses to ARQ 197 were phenocopied by RNAi-mediated c-Met depletion and further demonstrated by the growth inhibition of human tumors following oral administration of ARQ 197 in multiple mouse xenograft efficacy studies. Cumulatively, these data suggest that ARQ 197, currently in phase II clinical trials, is a promising agent for targeting cancers in which c-Met-driven signaling is important for their survival and proliferation. *Mol Cancer Ther; 9(6); 1544–53. ©2010 AACR.*

Introduction

A primary hurdle in developing anticancer therapeutics is to selectively target cancer cells while sparing normal tissues. c-Met is a receptor tyrosine kinase (RTK) that has low activity in normal tissues but is dysregulated in many tumor types. c-Met is the prototype member of a subfamily of RTKs, which includes Ron, that are structurally distinct from other RTK families. It is the only known high-affinity receptor for hepatocyte growth factor (HGF), also known as scatter factor (1–4). c-Met and HGF are both required for normal mammalian development (5). In adults, both c-Met and HGF are widely expressed in a variety of tissues; however, their expression is normally very low, confined to cells of epithelial or mesenchymal origin, and associated with tissue repair (6, 7). The results of *in vitro* and *in vivo* experiments show that this receptor-growth factor pair is involved in multiple physiologic cellular responses, including embryogenesis, cell proliferation, survival, differentiation, motility, and invasion (8).

Authors' Affiliations: [1]ArQule, Inc., Woburn, Massachusetts and [2]Boston Biomedical, Inc., Norwood, Massachusetts

Note: Supplementary material for this article is available at Molecular Cancer Therapeutics Online (http://mct.aacrjournals.org/).

N. Munshi, S. Jeay, Y. Li, and C-R Chen contributed equally to this manuscript.

Current address for S. Jeay: Novartis Institutes for Biomedical Research, Klybeckstrasse 141, CH-4057 Basel, Switzerland.

Corresponding Author: Dennis S. France, Department of Molecular Oncology, ArQule, Inc., 19 Presidential Way, Woburn, MA 01801. Phone: 781-994-0300; Fax: 781-994-0690. E-mail: dfrance@arqule.com

doi: 10.1158/1535-7163.MCT-09-1173

Increasing evidence suggests that tumorigenesis results from the subversion of normal signaling pathways. In particular, dysregulated RTKs are linked with various malignancies and represent a promising class of therapeutic targets for cancer treatment (9). In the 1980s, the RTK c-Met was discovered as an activated oncogene (10). Aberrant c-Met activity stimulates signaling pathways responsible for proliferation, invasion, migration, angiogenesis, survival, metastasis, and drug resistance. In contrast to *bona fide* growth factor signaling pathways such as epidermal growth factor receptor, c-Met signaling is functionally linked with both proliferation and metastatic phenotypes (11). Nonphysiologic c-Met activity may result from gene amplification, activating mutations, dimerization from overexpression, and autocrine or paracrine stimulatory mechanisms.

In *in vitro* studies, neoplastic cells can be stimulated to metastasize through constitutive c-Met signaling (12) and coexpression of c-Met and HGF in the tumor microenvironment seems to inform the molecular staging of human cancers (13). Ectopic HGF and c-Met overexpression have also been shown to drive tumorigenesis and metastasis in human xenograft tumor-bearing mice and transgenic mouse models (14). Subsequently, HGF or c-Met were found to be frequently overexpressed in many types of human solid tumors, including both sarcomas and carcinomas, as well as in associated metastases, for which the degree of c-Met expression correlates with poor patient prognosis (8). Activating c-Met mutations are described in sporadic and inherited forms of human renal papillary carcinomas (15), whereas genomic amplification of *met* is associated with gastric carcinoma (16, 17). Collectively, these data provide compelling evidence for the functional relevance of c-Met–activated networks in tumorigenesis

and metastatic progression, and underscore the importance of developing therapeutic strategies capable of interrupting c-Met signaling.

Multiple approaches have been used to block c-Met signaling, including c-Met biologics (ribozymes, dominant-negative receptors, decoy receptors, and peptides; 18–24), truncated HGF antagonist peptides (25, 26), and HGF antagonist antibodies (27, 28). The latter approaches, by definition, do not address ligand-independent c-Met activation and may only be effective for HGF-driven cancers. An indirect approach worthy of mention is the acceleration of c-Met degradation triggered by heat shock protein 90 inhibition, exemplified by 17-allylaminogeldanamycin (29). More recent efforts have focused on the development of low-molecular-weight inhibitors of HGF and c-Met (29–33).

We report the discovery of ARQ 197, a small molecule that selectively inhibits c-Met activity in cell-free and cell-based assays. c-Met–expressing cancer cell lines treated with ARQ 197 display either a dose-dependent loss of proliferative capacity or caspase-dependent apoptosis that positively correlates with either ligand-dependent c-Met activity or constitutively active c-Met. This study explores its effects in mice bearing HT29 (colon cancer), MKN-45 (gastric cancer), or MDA-MB-231 (breast cancer) xenografts.

Materials and Methods

Materials

Compound. ARQ 197 (Fig. 1), the designation for (–)-(3R,4R)-3-(5,6-dihydro-4*H*-pyrrolo[3,2,1-*ij*]quinolin-1-yl)-4-(1*H*-indol-3-yl)pyrrolidine-2,5-dione, was prepared as previously described (34). Reduction of the double bond by treatment with magnesium turnings in anhydrous methanol gave (±)-*trans*-3-(5,6-dihydro-4*H*-pyrrolo [3,2,1-*ij*] quinolin-1-yl)-4(1*H*-indol-3-yl) pyrrolidine-2,5-dione following silica gel chromatography. The single enantiomer (–)-(3R,4R)-3-(5,6-dihydro-4*H*-pyrrolo [3,2,1-*ij*] quinolin-1-yl)-4-(1*H*-indol-3-yl) pyrrolidine-2,5-dione was obtained by supercritical fluid chromatography.

Cell lines

Human cancer cell lines, unless otherwise noted, were purchased from the American Type Culture Collection and maintained according to guidelines (http://www.atcc.org/). MKN-45 gastric cancer cells were obtained from the Japanese Cancer Resource Bank and were grown as monolayers in DMEM supplemented with 10% fetal bovine serum (FBS) and maintained at 37°C in a humidified atmosphere at 5% CO_2. Recombinant human HGF and ZvAD-FMK (irreversible caspase inhibitor), used in all the studies, were purchased from R&D Systems.

Antibodies. Rabbit polyclonal antibodies included anti–phosphorylated c-Met (Tyr1349; Biosource International/Invitrogen Corp.), anti–c-Met (sc-10; Santa Cruz Biotechnology), anti–phosphorylated Akt (Ser473; Cell Signaling Technology), anti-Akt (Cell Signaling Technology), anti-phosphorylated Erk-1/2 (Thr202/Tyr204; Cell Signaling Technology), anti-Erk-1/2 (Cell Signaling Technology), anti–phosphorylated signal transducer and activator of transcription 3 (STAT-3; Tyr705; Cell Signaling Technology), and anti–STAT-3 (Cell Signaling Technology). The monoclonal antibody against β-actin was obtained from Invitrogen Corp.

Common methods

Western blot analyses. Whole-cell extracts were prepared in Cell Lysis Buffer (Cell Signaling Technology) containing 20 mmol/L Tris-HCl (pH 7.5), 150 mmol/L NaCl, 1 mmol/L Na_2EDTA, 1 mmol/L EGTA, 1% Triton, 2.5 mmol/L sodium pyrophosphate, 1 mmol/L β-glycerophosphate, 1 mmol/L Na_3VO_4, 1 μg/mL leupeptin, and 1 mmol/L phenylmethane sulphonyl fluoride. The protein concentration was measured using a Bradford assay and the Bio-Rad reagent (Bio-Rad) according to the manufacturer's instructions. Samples (50 μg of total protein) were resolved by SDS-7.5% PAGE under reducing conditions and transferred onto polyvinylidene difluoride membranes (Millipore Corp.). The membranes were incubated overnight at 4°C in TBS-T [50 mmol/L Tris-HCl (pH 7.6), 200 mmol/L NaCl, 0.1% Tween 20] with 3% bovine serum albumin. Proteins were detected by incubation with the specific antibody in TBS-T with 3% bovine serum albumin. After extensive washing in TBS-T, a 1:5,000 dilution of secondary horseradish peroxidase–conjugated antibody (Amersham Biosciences Corp.) was added for 1 hour and specific protein bands were visualized by using an enhanced chemiluminescence detection system (Perkin-Elmer Detection Systems) according to the manufacturer's instructions.

c-Met small interfering RNA and transfection

Small interfering RNAs (siRNA) targeting *met* or *gapdh* mRNA were obtained from Dharmacon, Inc., and used according to the manufacturer's instructions. Briefly, a pool of four *met*-specific 21-nucleotide RNA oligonucleotides forming a 19-bp duplex core with 2-nucleotide 3 overhang was used in combination. siRNA duplexes were transiently transfected into the indicated cells using the DharmaFECT 4 reagent according to the manufacturer's instructions (Dharmacon, Inc.). Transfection of a nontargeting siRNA under the same conditions was undertaken in parallel as a control.

Specific methods

Kinase profiling. The activity of ARQ 197, at a concentration of 5 or 10 μmol/L using an ATP concentration of 10 μmol/L, was screened against a protein kinase panel of 230 human protein kinases by Millipore using the Millipore KinaseProfiler Selectivity Testing Service. Protocols are available at http://www.millipore.com/drugdiscovery/dd3/assayprotocols.

c-Met SDS-PAGE *in vitro* kinase assay

Recombinant c-Met protein (100 ng) purchased from Millipore was preincubated with increasing

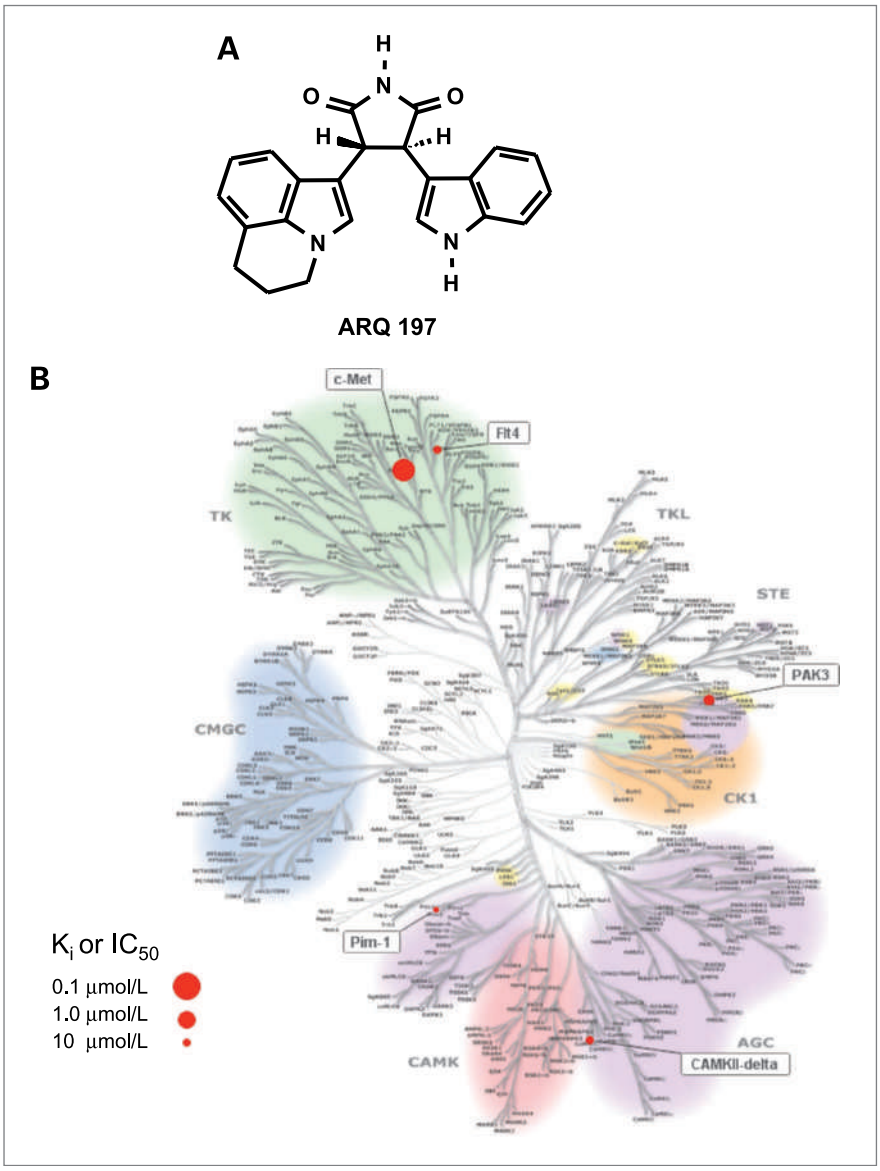

Figure 1. A, chemical structure of ARQ 197. B, kinase profiling of ARQ 197 against 230 human kinases. The inhibitory effect of ARQ 197 was profiled against 230 human kinases at Millipore Corp. The sizes of the red circles on the kinome tree are proportional to the potency determined by repeat dose-response follow-up inhibition studies against the top five kinases inhibited by ARQ 197. The K_i of 355 nmole/L for ARQ 197 against c-Met was derived from the kinetic radiometric filtermat assay. Kinome tree used by permission from Cell Signaling Technology, (http://www.cellsignal.com).

concentrations of ARQ 197 for 30 minutes at room temperature. Following preincubation, 100 μmol/L of poly-Glu-Tyr substrate and various concentrations of ATP containing 5 μCi of [γ-^{32}P]ATP were added to the reaction mixture. The reaction was incubated for 5 minutes at room temperature and then stopped by the addition of 5 μL of SDS-polyacrylamide gel, reducing sample buffer. The samples were then loaded onto a 7.5% acrylamide gel and SDS-PAGE was performed. The phosphorylated poly-Glu-Tyr substrates were ultimately visualized by autoradiography. c-Met activity was quantified by densitometry using the Scion Image software.

c-Met filtermat kinetic assays

Recombinant c-Met protein (50 ng) comprising residues 974 to 1390 (Millipore) was incubated in a reaction buffer [50 mmol/L Tris-HCl (pH 7.5), 2 mmol/L DTT, 0.1 mmol/L Na_3VO_4, 10 mmol/L $MgCl_2$, 1 mmol/L EGTA, 0.02 mg/mL bovine serum albumin, and 10% glycerol] with various concentrations of ARQ 197 or DMSO in a total volume of 20 μL. After incubating for 20 minutes at room temperature, 20 μL of 20 μmol/L poly-Glu-Tyr substrate and 20 μL of increasing amounts of cold ATP containing 1.5 μCi of [γ-^{33}P]ATP were added to initiate the reaction. The reaction was stopped after 5, 10, 20, 40, and 60 minutes by the addition of 10% phosphoric acid and 10 μL aliquots of the reaction mixture were spotted onto P30 filtermat in triplicate. The filters were washed thrice for 5 minutes with 0.75% phosphoric acid and once with methanol for 2 minutes. The level of radioactivity was determined by using a Wallac TriLux MicroBeta liquid scintillation

counter. Nonspecific binding was determined by conducting the assay in the absence of enzyme and then subtracting the value from each of the experimental values. Reaction rates were determined in the linear range of each reaction and GraphPad Prism software was used to calculate the K_m and V_{max} values.

c-Met phosphorylation and downstream c-Met–dependent signaling pathways

HT29, MKN-45, MDA-MB-231, and NCI-H441 (lung cancer) human cancer cells were used to assess the effect of ARQ 197 on c-Met phosphorylation and c-Met–dependent signaling pathways. Cells were cultured in low-serum medium (0.5% FBS) in the presence or absence of ARQ 197 for 24 hours before being stimulated or not stimulated with 100 ng/mL recombinant human HGF for 10 minutes before cell lysis. Phosphorylation and expression levels of both c-Met and its downstream signaling molecules Akt, Erk-1/2, and STAT-3 were assessed by Western blotting with specific antibodies.

Cell proliferation assay

Cells were seeded in 96-well plates overnight in a medium with 10% FBS. Each cell line was optimized for seeding cell number to ensure a similar degree of confluence at the end of the experiment in nontreated (control) wells. The next day, cells were treated with different concentrations of ARQ 197 for 24 hours at 37°C. After ARQ 197 treatment, the drug-containing medium was removed, and cells were washed twice with PBS and incubated in a drug-free medium for an additional 48 hours. Cells were then incubated and stained for 4 hours with the MTS reagent (final concentration of 0.5 mg/mL; Promega) per well and were lysed. The results were quantitated by spectrophotometry at λ = 450 nm.

Apoptosis induction assays

HT29, MKN-45, and MDA-MB-231 cells were plated in black 96-well plates at 5,000 cells per well overnight in a medium with 10% FBS. The next day, cells were treated with increasing concentrations of ARQ 197 (0.03–10 μmol/L) for 24, 32, and 48 hours at 37°C. After ARQ 197 treatment, the drug-containing medium was removed and cells were incubated for at least 10 minutes in a labeling solution (10 mmol/L HEPES, 140 mmol/L NaCl, and 6 mmol/L $CaCl_2$) containing 2 μg/mL Hoescht 33342 (blue channel; Molecular Probes/Invitrogen Corp.), 500-times diluted Annexin V-FITC (green channel; Roche Applied Science), and 1 μg/mL propidium iodide (red channel; Roche Applied Science). High-content image acquisition and analysis were carried out using a Beckman Coulter IC100 Cytometer. The program was set to take four images per well. The exposure time was set at 16.7 ms/10% gain, 500 ms/35% gain, and 300 ms/30% gain for the 4,6-diamidino-2-phenylindole, FITC, and rhodamine channels, respectively. Images were processed and the numbers of positive cells for each channel and each condition were determined using the Cytoshop 2.1 software (Beckman Coulter, Inc.). In addition, HT29 cells were treated with increasing concentrations of ARQ 197 for 32 hours in the absence or the presence of 25, 50, and 100 μmol/L ZvAD-FMK (irreversible general caspase inhibitor), and the same procedures were undertaken. All experiments were done in triplicate.

To determine whether the apoptotic effect was due to c-Met inhibition, the effect of ARQ 197 when glyceraldehyde-3-phosphate dehydrogenase (GAPDH) and c-Met were knocked down using siRNA was investigated. HT29, MKN-45, and MDA-MB-231 cells were transfected with a nontargeted control siRNA, a *gapgh*-targeted control siRNA, or a *met*-targeted siRNA. After 3 days, c-Met, GAPDH, and β-actin expression levels were determined using specific antibodies. To determine if the effect was caspase dependent, HT29, MKN-45, and MDA-MB-231 cells were transfected with a *met*-targeted siRNA for 2 days and incubated in the absence or the presence of increasing concentrations of ZvAD-FMK for 1 additional day. A nontargeted siRNA and a *gapgh*-targeted siRNA (siRNA GAPDH) were also transfected in parallel, as controls. Cells were then stained with Annexin V-FITC and propidium iodide, and the percentage of apoptotic cells was determined. Experiments were done in triplicate.

Xenograft studies

Female athymic nude mice (Charles River Laboratory) were acclimated to the animal housing facility for at least 1 week before the study. All experimental procedures conformed to the guiding principles of the ArQule Institutional Animal Care and Use Committee. Efficacy studies were done in athymic mice bearing HT29, MKN-45, or MDA-MB-231 tumor xenografts to determine the effect of ARQ 197 on tumor growth. Tumor cells [5×10^6 (HT29) and 8×10^6 (MKN-45 and MDA-MB-231) cells/animal] were inoculated s.c. on day 0. Tumor dimensions were measured by a digital caliper and tumor volumes were calculated as length × width^2/2. When tumors reached a volume of ~100 mm^3, mice were randomized into groups and treated daily with orally administered vehicle control or 200 mg/kg ARQ 197 formulated in polyethylene glycol 400/20% Vitamin E tocopheryl polyethylene glycol succinate (60:40) at 30 mg/mL, for 5 consecutive days, followed by a 2-day dosing holiday for four cycles. Therefore, each animal received a total of 20 doses. Results are expressed as mean tumor volume ± SEM. To assess differences in tumor size between groups, a Mann-Whitney nonparametric *t* test was performed and significance was defined as $P < 0.05$.

Immunohistochemistry

Athymic mice with established subcutaneous HT29 human colon cancer were given ARQ 197 (200 mg/kg) or vehicle control. The tumors were dissected 4 and 24 hours after dosing and were formalin-fixed and

processed for standard immunohistochemistry analysis of 6-μm-thick sections. Phospho-c-Met was detected using an anti–phospho-c-Met antibody recognizing the phosphotyrosine 1349 of c-Met (Biosource) and visualized with an immunoperoxidase system using diaminobenzidine, which yields an insoluble brown reaction product (Super-Sensitive IHC system, BioGenex).

Pharmacokinetics

Pharmacokinetic studies were conducted using 8-week-old female athymic (Ncr *nu/nu*) mice (n = 24) from Charles River Laboratories of ~25 g in weight. Animals were fasted overnight and dosed the following morning by oral gavage with 200 mg/kg ARQ 197 formulated with polyethylene glycol 400/Vitamin E. All 24 mice were dosed and blood samples (n = 3 mice per time point) were collected through cardiac puncture either immediately before dosing or 0.25, 0.5, 1, 2, 4, 8, and 10 hours after dosing with ARQ 197 into tubes containing potassium EDTA. Plasma was collected from the blood samples by centrifugation at 1,500 × g for 10 minutes and stored at −80°C until analysis for ARQ 197 content by liquid chromatography tandem mass spectrometry. Noncompartmental pharmacokinetic parameters were calculated from plasma concentration-time data using the WinNonlin software (Pharsight).

Results

Identification of ARQ 197 as a selective inhibitor of c-Met activity

ARQ 197 (Fig. 1A) was discovered by a phenotype-driven process to identify cancer survival pathway inhibitors in metastatic cancer cell lines, which was optimized using pathway-based assays. Subsequent experiments identified c-Met as the molecular target of ARQ 197.

The selectivity of ARQ 197 against c-Met kinase activity was observed when this compound was profiled against a protein kinase panel of 230 human kinases. Only 4 of the other 229 kinases in this panel showed any detectable inhibition by ARQ 197 (Fig. 1B). In this screening assay, no inhibition was observed for the vast majority of RTKs tested, including epidermal growth factor receptor, insulin receptor, platelet-derived growth factor receptor α, and fibroblast growth factor receptor 1 and 4. Ron kinase, which belongs to the c-Met family of RTKs, was not inhibited by ARQ 197 at 10 μmol/L under the conditions of these assays and showed only modest inhibition (35%) at a concentration of 30 μmol/L.

To examine the biochemical mode of inhibition of ARQ 197, kinetic analyses were done using recombinant human c-Met in a filtermat-based assay. The K_m of ATP was 50.5 ± 2.2 μmol/L (Supplementary Table S1; Supplementary Fig. S1), which is similar to the K_m value

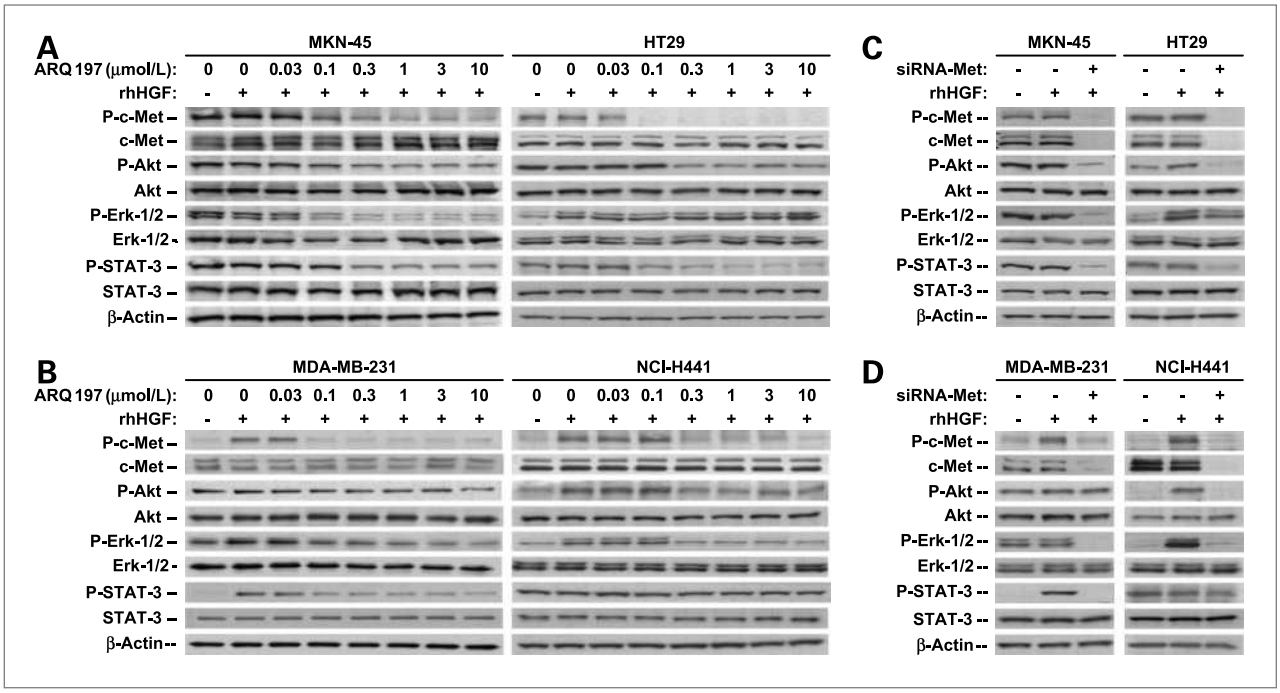

Figure 2. Effect of ARQ 197 on c-Met phosphorylation and signal transduction pathways in MNK-45, HT29, MDA-MB-231, and NCI-H441 cells. A and B, cells were starved in medium containing 0.5% FBS in the absence or presence of increasing concentrations of ARQ 197 for 24 h and stimulated with 100 ng/mL human recombinant HGF 10 min before cell lysis. Western blotting was performed for each protein or phosphoprotein using specific antibodies as described. C and D, cells were transfected with a control siRNA or a *met*-targeted siRNA for 2 d, before cells were starved in medium containing 0.5% FBS for an additional 24 h and stimulated with 100 ng/mL human recombinant HGF for 10 min. Western blotting was performed for each protein or phosphoprotein as in A and B for direct comparison.

of ATP determined previously (35). Although the addition of increasing concentrations of ARQ 197 did not significantly affect the K_m of ATP, exposure of c-Met to 0.5 μmol/L ARQ 197 decreased the V_{max} of c-Met by ~3-fold (Supplementary Table S1; Fig. 2). The ability of ARQ 197 to decrease the V_{max} without affecting the K_m of ATP confirmed that ARQ 197 inhibits c-Met through a non–ATP-competitive mechanism and may therefore account for its high degree of kinase selectivity. In these kinetic studies, ARQ 197 inhibited human recombinant c-Met with a calculated inhibitory constant (K_i) of ~ 355 nmol/L. Although the highest concentration of ATP used in these studies was 200 μmol/L, the potency of ARQ 197 against c-Met in this assay format was not reduced by using concentrations of ATP up to 1 mmol/L (data not shown).

ARQ 197 inhibits c-Met phosphorylation and downstream c-Met signaling pathways

HT29, MKN-45, MDA-MB-231, and NCI-H441 human cancer cells were used to assess the effect of ARQ 197 on c-Met phosphorylation and c-Met–dependent signaling pathways. *In vitro* exposure to ARQ 197 inhibited constitutive c-Met phosphorylation in HT29 and MKN-45 cells (Fig. 2A), and HGF-induced c-Met phosphorylation in MDA-MB-231 and NCI-H441 cells (Fig. 2B) with an IC_{50} of 100 to 300 nmol/L.

Although the constitutive phosphorylation of Akt, Erk-1/2, and STAT-3 pathways were each inhibited by ARQ 197 in MKN-45 cells (Fig. 2A, left), these pathways downstream of c-Met were differentially affected in the three other cell lines tested (Fig. 2A, right, and B). In HT29 cells, c-Met inhibition correlated with the decrease of Akt and STAT-3, but not with Erk-1/2 phosphorylation (Fig. 2A, right). In contrast, in MDA-MB-231 cells, ARQ 197-mediated c-Met inhibition led to limited reduction in Erk-1/2 phosphorylation, whereas STAT-3 phosphorylation mirrored that of c-Met (Fig. 2B, left). In NCI-H441 cells, both Erk-1/2 and Akt phosphorylation followed that of c-Met, but not STAT-3 (Fig. 2B, right).

To further explore the role of c-Met in the activation of the Akt, Erk-1/2, and STAT-3 signaling pathways, siRNAs were used to specifically inhibit c-Met expression in these cells. Transfection of c-Met–targeted siRNA decreased c-Met protein expression by at least 90% and, as expected, inhibited both constitutive (Fig. 2C) and HGF-induced c-Met phosphorylation (Fig. 2D) in these cancer cells. Importantly, c-Met depletion (Fig. 2C and 2D) yielded a pattern of pathway inhibition that was remarkably similar to that observed following ARQ 197 treatment (Fig. 2A and 2B). Together, these data strongly suggest that ARQ 197 inhibits constitutive and ligand-mediated c-Met autophosphorylation and, by extension, c-Met activity, in turn leading to the inhibition of downstream c-Met effectors. The cell type–specific repertoire of signaling pathways driven by c-Met was, as expected, dependent on the genetic background of the specific cell line used (36).

Table 1. Antiproliferative activity of ARQ 197 against various human cancer cell lines: dependence on c-Met status

Human cancer cell line	Tumor origin	c-Met status	Cytotoxicity IC_{50} (μM)
SK-MEL-28	Melanoma	–	>33
NCI-H661	NSCLC	–	>33
NCI-H446	SCLC	–	7.00
MDA-MB-231	Breast Ca	+	0.55
DLD-1	Colon Ca	+	0.53
A549	NSCLC	+	0.59
SK-OV-3	Ovarian Ca	+	0.66
NCI-H460	NSCLC	+	0.60
A375	Melanoma	+	0.42
NCI-H441	NSCLC	+	0.30
HT29	Colon Ca	+	0.49
MKN-45	Gastric Ca	+	0.58

NOTE: A total of 12 human cancer cell lines with either confirmed expression of c-Met (+) or confirmed lack of c-Met protein (–) were treated with increasing concentrations of ARQ 197 for 24 hours and were grown in compound-free medium for an additional 48 hours. Cell proliferation was measured using an MTS assay as described. Anti-proliferative potencies of ARQ 197 for each cell line are indicated (IC_{50}). The results shown are representative of at least eight independent experiments.
Abbreviations: NSCLC, non-small cell lung cancer; SCLC, small cell lung cancer.

c-Met status and cytotoxic sensitivity to ARQ 197 in monolayer cultures of human cell lines

Multiple cancer cell lines were screened for their sensitivity to ARQ 197. Twelve human cancer cell lines representing various tumor types were treated with ARQ 197 at concentrations ranging from 0.03 to 30 μmol/L (Table 1). In the human cell lines with no immunodetectable c-Met or phospho-c-Met, ARQ 197 treatment exerted little, if any, antiproliferative effect (cytotoxicity IC_{50} values of >30 μmol/L for both the SK-MEL-28 and NCI-H661 cancer cell lines, and 7.0 μmol/L for the NCI-H446 cell line). In contrast, cancer cell lines harboring c-Met and expressing phospho-c-Met to varying degrees showed submicromolar sensitivity to ARQ 197 in this standard cytotoxicity assay, exhibiting at least a 10-fold to a >100-fold greater sensitivity to the antiproliferative effects of ARQ 197 compared with c-Met null human cancer cell lines (Table 1).

ARQ 197 induction of caspase-dependent apoptosis is increased in c-Met–expressing human cancer cells

The ability of ARQ 197 to induce cell death was assessed using HT29, MKN-45, and MDA-MB-231 cells to determine whether these effects represented cell death or

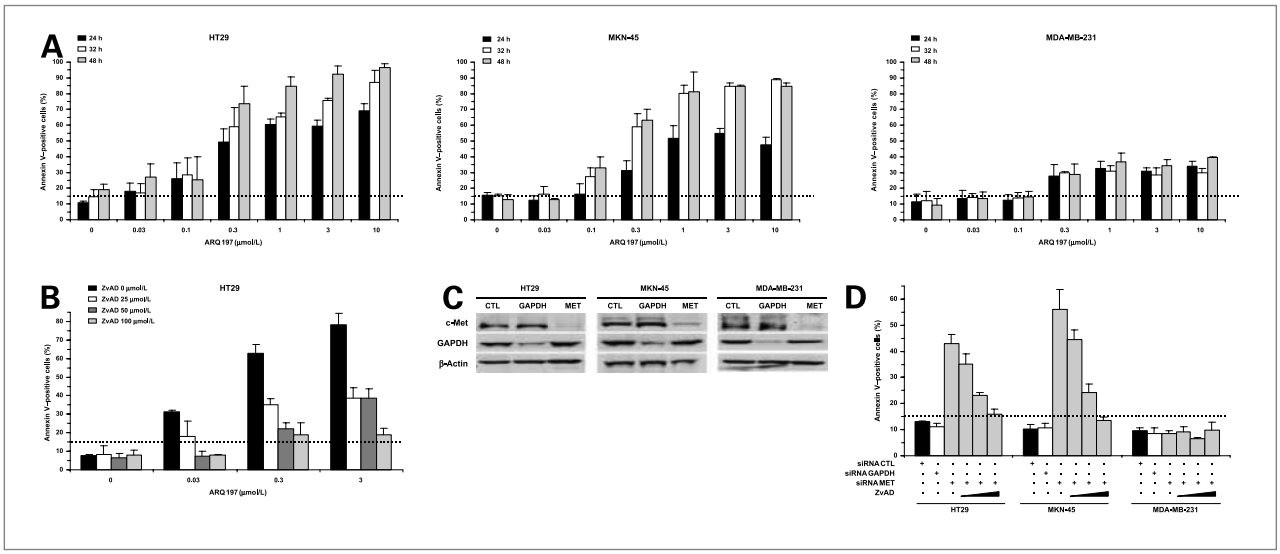

Figure 3. Effect of ARQ 197 on apoptosis of human cancer cells. A, ARQ 197 induces apoptosis in a cell type–specific manner. HT29, MKN-45, and MDA-MB-231 cells were treated with increasing concentrations of ARQ 197 for 24, 32, and 48 h. Cells were then stained with Annexin V-FITC and propidium iodide, and the percentage of apoptotic cells was determined as described. Experiments were done in triplicate. Columns, mean; bars, SD. B, ARQ 197-mediated induction of apoptosis is caspase dependent. HT29 cells were treated with increasing concentrations of ARQ 197 for 32 h in the absence or the presence of 25, 50, and 100 μmol/L ZvAD-FMK irreversible general caspase inhibitor. Cells were then stained with Annexin V-FITC and propidium iodide, and the percentage of apoptotic cells was determined. Experiments were done in triplicate. Columns, mean; bars, SD. C, effective knockdown of GAPDH and c-Met using siRNA. HT29, MKN-45, and MDA-MB-231 cells were transfected with a nontargeted control siRNA (CTL), a *gapgh*-targeted control siRNA (GAPDH), or a *met*-targeted siRNA (MET). After 3 d, c-Met, GAPDH, and β-actin expression levels were determined using specific antibodies. D, selective caspase-dependent apoptosis of HT29 and MKN-45 cells after siRNA-mediated knockdown of c-Met. HT29, MKN-45, and MDA-MB-231 cells were transfected with a *met*-targeted siRNA (siRNA MET) for 2 d and incubated in the absence or the presence of increasing concentrations of ZvAD-FMK for 1 additional day. A nontargeted siRNA (siRNA CTL) and a *gapgh*-targeted siRNA (siRNA GAPDH) were also transfected in parallel, as controls. Cells were then stained with Annexin V-FITC and propidium iodide, and the percentage of apoptotic cells were determined. Experiments were done in triplicate. Columns, mean; bars, SD.

growth arrest. Exposure to ARQ 197 significantly increased the percentage of Annexin V–positive cells (85–90%) in HT29 and MKN-45 cell lines (Fig. 3A, left and middle). In contrast, in MDA-MB-231 cells—a more modest induction of apoptosis, up to a maximum of 35%—was observed following ARQ 197 treatment (Fig. 3A, right). ARQ 197 failed to increase propidium iodide incorporation significantly after 24 to 48 hours of treatment in MDA-MB-231 (data not shown). In addition, the levels of apoptosis in HT29 cells induced by ARQ 197 were reduced by ZvAD-FMK, a general and irreversible caspase inhibitor (Fig. 3B). Overall, these findings suggest that cancer cell sensitivity directly links to the ability of ARQ 197 to induce cell death by the caspase-dependent intrinsic apoptotic pathway.

To confirm that the differential effects of ARQ 197 relate to its effect on c-Met, HT29, MKN-45, and MDA-MB-231 cells were transfected with siRNA, targeting the *met* receptor transcript. Specific and effective c-Met depletion was demonstrated by Western blotting (Fig. 3C). To control for nonspecific effects on cell proliferation, siRNA targeting the *gapdh* transcript was also tested (Fig. 3C). As expected, transfections of nontargeting siRNA or *gapdh*-targeted siRNA did not induce apoptosis (Fig. 3D). Consistent with the effect of ARQ 197, a marked increase in apoptosis was evident following c-Met depletion, using *met*-targeted siRNA, in HT29 and MKN-45 cells, whereas no effect was observed in MDA-MB-231 cells (Fig. 3D). The presence of ZvAD-FMK inhibited apoptotic induction by c-Met depletion in HT29 and MKN-45 cells (Fig. 3D). These data confirm that the differential sensitivity of human cancer cells to ARQ 197 is linked to its inhibitory effect on c-Met and c-Met–dependent signaling pathways. Overall, these findings support the hypothesis that cancer cells expressing activated c-Met should be sensitive to caspase-dependent apoptosis induced by ARQ 197.

In vivo antitumor activity of ARQ 197

To test the antitumor activity of ARQ 197, xenograft mouse models using HT29, MKN-45, and MDA-MB-231 human cancer cell lines were evaluated. All three xenograft models showed a reduction in tumor growth: 66% ($P = 0.01$) in the HT29 model, 45% ($P = 0.02$) in the MKN-45 model, and 79% ($P < 0.05$) in the MDA-MB-231 model (Fig. 4A). In these xenograft studies, no significant body weight changes following oral administration of ARQ 197 at 200 mg/kg were observed. Pharmacodynamically, the phosphorylation of c-Met in human colon xenograft tumors (HT29) was strongly inhibited by ARQ 197, as assessed by a dramatic reduction of c-Met autophosphorylation 24 hours after a single oral

dose of 200 mg/kg of ARQ 197. This same dosage in mice showed that tumor xenografts were exposed to sustained plasma levels of ARQ 197, consistent with the observed pharmacodynamic inhibition of c-Met phosphorylation and inhibition of proliferation of c-Met harboring cancer cell lines. A C_{max} of 5.73 μg/mL (13 μmol/L), an area under the concentration-time curve of 12.1 μg mL^{-1} h, and a $t_{1/2}$ of 2.4 hours were measured. Plasma levels of ARQ 197 10 hours after dosing were determined to be 1.3 μmol/L, >3-fold above the biochemical inhibitory constant of ARQ 197 for c-Met. This study showed that ARQ 197 was able to suppress its target *in vivo* in the xenografted human tumor tissue (Fig. 4B). Finally, these *in vivo* data confirm the hypothesis generated from *in vitro* cellular data that ARQ 197 inhibits the growth of c-Met–dependent xenografted human tumors.

Discussion

ARQ 197 is a novel and highly selective c-Met tyrosine kinase inhibitor; it inhibited c-Met with a K_i of 355 nmol/L and had no appreciable inhibitory effect against the majority of the other 229 human kinases in the panel, including Ron kinase, which belongs to the same family of kinases as c-Met (Fig. 1). In addition, the mode of inhibition of ARQ 197 is not competitive with respect to ATP (Supplementary Fig. S1). This feature of ARQ 197 distinguishes it from all the publicly disclosed c-Met inhibitors in clinical and preclinical development, most of which have been reported to be ATP competitive (37, 38). Although a K_i value of 355 nmol/L suggests that ARQ 197 is not as potent as other c-Met inhibitors under development, the pharmacokinetic suppression, pathway inhibition, and antiproliferative effects in cellular assays are in the same range as the biochemical potency, differentiating it from what is typically obtained for an ATP-competitive inhibitor. ARQ 197 disrupts constitutive and ligand-mediated (HGF) c-Met phosphorylation and in turn inhibits the downstream c-Met effectors *in vitro* (Fig. 2). Those cancer cell lines with constitutive c-Met activity, exemplified by MKN-45 and HT29, were sensitive to ARQ 197 and showed caspase-dependent apoptosis. Furthermore, siRNA-mediated c-Met depletion phenocopied the pharmacodynamic effects of ARQ 197 on cancer cells, reinforcing the hypothesis that c-Met is the primary target of the antiproliferative and proapoptotic effects of ARQ 197. Finally, oral dosing of ARQ 197 significantly inhibited tumor growth in human xenograft tumor–bearing mice at doses that were well tolerated.

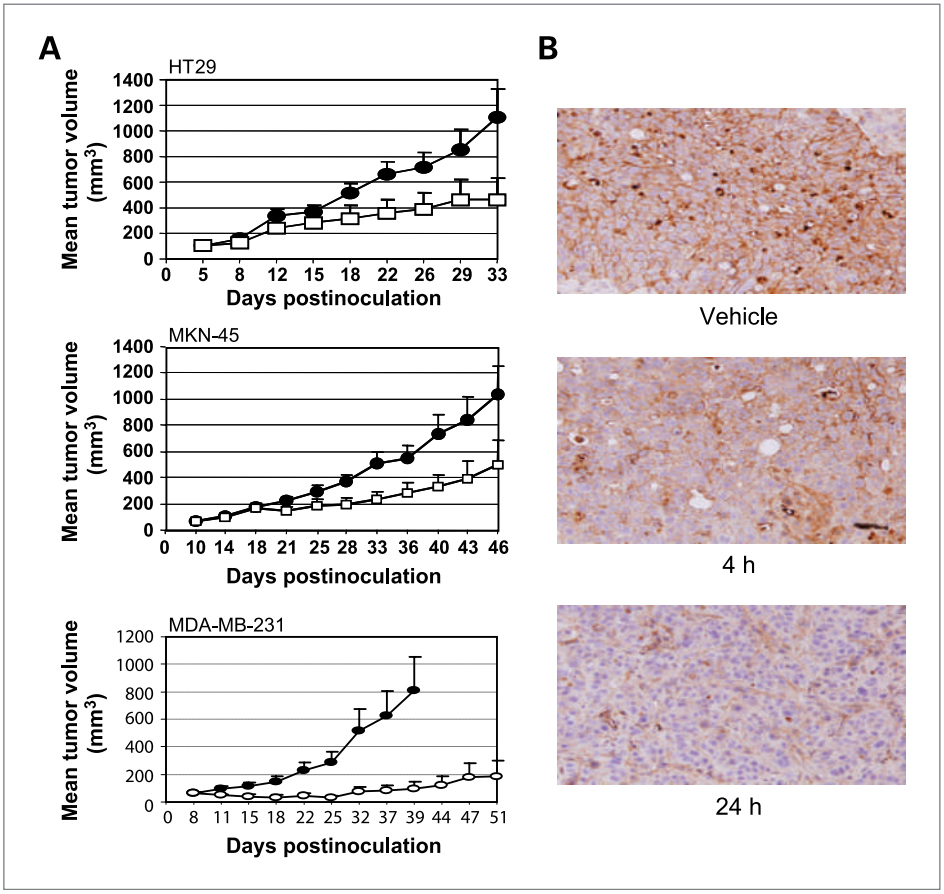

Figure 4. ARQ 197 inhibits tumor growth in human tumor xenograft models. Immunosuppressed mice with established subcutaneous HT29 human colon tumors, MKN-45 human gastric tumors, or MDA-MB-231 breast tumors were dosed orally with 200 mg/kg ARQ 197 or vehicle control. All regimens were administered daily for 5 d (Monday to Friday), with a 2-d drug holiday for four cycles, for a total number of 20 treatments. A, tumor size was evaluated periodically during treatment at the indicated days postinoculation. Points, mean of tumor volume in mm^3 of several tumors (n = 8 for HT29 and MKN-45; n = 10 for MDA-MB-231) during the course of the treatment period; bars, SEM. B, phospho-c-Met was detected in histopathologic samples 24 h after dosing HT29 tumor–bearing mice with a single dose of ARQ 197 (200 mg/kg). Phospho-c-Met was visualized with the use of an immunoperoxidase system using diaminobenzidine, which yields an insoluble brown reaction product.

Cancer cells with constitutive c-Met activation, including one with *met* gene amplification (MKN45), underwent apoptosis following interruption of c-Met signaling by either siRNA-mediated c-Met depletion or ARQ 197 inhibition in this study (Fig. 3A). In contrast, a cancer cell line with ligand-dependent c-Met activity, exemplified by the MDA-MB-231 cell line, underwent cytostasis and was less susceptible to apoptosis induction by ARQ 197 *in vitro*. Nonetheless, all three of these respective cell lines were responsive to ARQ 197 *in vivo* in corresponding xenograft models, as shown by a reduction in tumor growth. This suggests that the inhibition of c-Met by ARQ 197 will exert its antitumor effect across a broad spectrum of c-Met–driven tumors, regardless of the mode of c-Met activation.

Cancer cells without detectable c-Met protein and mRNA were markedly less sensitive (10- to 100-fold) to the cytotoxic effects of ARQ 197 than those expressing c-Met (Table 1). Human cancer cell lines expressing c-Met activity seem exquisitely sensitive in tumor xenograft models, with the clear inhibition of tumor growth documented after a regimen of orally administered ARQ 197. In addition, in the HT29 xenograft model, a single dose of ARQ 197 induced a reduction in immunodetectable phosphorylated c-Met (Fig. 4C). These data support the hypothesis that c-Met signaling is a primary therapeutic target for ARQ 197 *in vivo*.

To date, no c-Met effectors have been identified that will predict the cells or tumors most likely to respond to therapeutic c-Met intervention strategies. This could be explained by the variable inhibition of downstream c-Met signaling pathways and cross-talk with other signaling pathways (39). Alternatively, the presence of other cancer cell mutations may facilitate alternate mechanisms for survival. In addition, the local cellular microenvironment may influence the degree to which tumor cells rely on c-Met–driven signaling (8). Cancer cells exhibiting genomic c-Met amplification seem acutely sensitive to c-Met–targeted therapeutics, suggesting c-Met amplification as a potential predictive marker (40); however, other than in gastric cancer, genomic *met* amplification seems relatively rare. Phase I clinical studies have shown that ARQ 197 is well tolerated and has encouraging antitumor activity (41–43). Clinical data from ongoing phase II studies with ARQ 197 will be evaluated critically to determine whether patient stratification based on the expression of c-Met and/or phospho-c-Met or its downstream effectors will be useful in predicting the efficacy of ARQ 197 for the treatment of human cancers.

Collectively, the data generated in this study justify further investigation of the therapeutic potential of ARQ 197, the first selective c-Met inhibitor, for the treatment of human cancers in which c-Met–driven signaling plays an important role in survival and proliferation.

Disclosure of Potential Conflicts of Interest

All authors own stock in ArQule, Inc. All authors were employed by ArQule, Inc., when the work was done, and all work described herein was conducted at ArQule, Inc. The senior author C.J. Li is the former chief scientific officer of ArQule, Inc.

Acknowledgments

We thank Dr. Brian Schwartz, chief medical officer of ArQule, Inc., for critically reviewing this manuscript, the present and former members of ArQule's research team who worked on this project, and our scientific advisors for their help and advice during this project.

Grant Support

ArQule, Inc.
The costs of publication of this article were defrayed in part by the payment of page charges. This article must therefore be hereby marked *advertisement* in accordance with 18 U.S.C. Section 1734 solely to indicate this fact.

Received 12/16/2009; revised 03/05/2010; accepted 03/30/2010; published OnlineFirst 05/18/2010.

References

1. Bottaro DP, Rubin JS, Faletto DL, et al. Identification of the hepatocyte growth factor receptor as the c-met proto-oncogene product. Science 1991;251:802–4.
2. Gherardi E, Stoker M. Hepatocytes and scatter factor. Nature 1990; 346:228.
3. Naldini L, Weidner KM, Vigna E, et al. Scatter factor and hepatocyte growth factor are indistinguishable ligands for the MET receptor. EMBO J 1991;10:2867–78.
4. Weidner KM, Arakaki N, Hartmann G, et al. Evidence for the identity of human scatter factor and human hepatocyte growth factor. Proc Natl Acad Sci U S A 1991;88:7001–5.
5. Birchmeier C, Gherardi E. Developmental roles of HGF/SF and its receptor, the c-Met tyrosine kinase. Trends Cell Biol 1998;8: 404–10.
6. Di Renzo MF, Narsimhan RP, Olivero M, et al. Expression of the Met/HGF receptor in normal and neoplastic human tissues. Oncogene 1991;6:1997–2003.
7. Sonnenberg E, Meyer D, Weidner KM, Birchmeier C. Scatter factor/hepatocyte growth factor and its receptor, the c-met tyrosine kinase, can mediate a signal exchange between mesenchyme and epithelia during mouse development. J Cell Biol 1993;123:223–35.
8. Birchmeier C, Birchmeier W, Gherardi E, Vande Woude GF. Met, metastasis, motility and more. Nat Rev Mol Cell Biol 2003;4:915–25.
9. Blume-Jensen P, Hunter T. Oncogenic kinase signalling. Nature 2001;411:355–65.
10. Cooper CS, Park M, Blair DG, et al. Molecular cloning of a new transforming gene from a chemically transformed human cell line. Nature 1984;311:29–33.
11. Boccaccio C, Comoglio PM. Invasive growth: a MET-driven genetic programme for cancer and stem cells. Nat Rev Cancer 2006;6: 637–45.
12. Boccaccio C, Sabatino G, Medico E, et al. The MET oncogene drives a genetic programme linking cancer to haemostasis. Nature 2005; 434:396–400.
13. Kammula US, Kuntz EJ, Francone TD, et al. Molecular co-expression of the c-Met oncogene and hepatocyte growth factor in primary colon cancer predicts tumor stage and clinical outcome. Cancer Lett 2007;248:219–28.

14. Takayama H, LaRochelle WJ, Sharp R, et al. Diverse tumorigenesis associated with aberrant development in mice overexpressing hepatocyte growth factor/scatter factor. Proc Natl Acad Sci U S A 1997; 94:701–6.
15. Danilkovitch-Miagkova A, Zbar B. Dysregulation of Met receptor tyrosine kinase activity in invasive tumors. J Clin Invest 2002;109: 863–7.
16. Nakajima M, Sawada H, Yamada Y, et al. The prognostic significance of amplification and overexpression of c-met and c-erb B-2 in human gastric carcinomas. Cancer 1999;85:1894–902.
17. Schmidt L, Duh FM, Chen F, et al. Germline and somatic mutations in the tyrosine kinase domain of the MET proto-oncogene in papillary renal carcinomas. Nat Genet 1997;16:68–73.
18. Abounader R, Lal B, Luddy C, et al. *In vivo* targeting of SF/HGF and c-met expression via U1snRNA/ribozymes inhibits glioma growth and angiogenesis and promotes apoptosis. FASEB J 2002;16:108–10.
19. Firon M, Shaharabany M, Altstock RT, et al. Dominant negative Met reduces tumorigenicity-metastasis and increases tubule formation in mammary cells. Oncogene 2000;19:2386–97.
20. Furge KA, Kiewlich D, Le P, et al. Suppression of Ras-mediated tumorigenicity and metastasis through inhibition of the Met receptor tyrosine kinase. Proc Natl Acad Sci U S A 2001;98:10722–7.
21. Herynk MH, Stoeltzing O, Reinmuth N, et al. Down-regulation of c-Met inhibits growth in the liver of human colorectal carcinoma cells. Cancer Res 2003;63:2990–6.
22. Jiang WG, Grimshaw D, Lane J, et al. A hammerhead ribozyme suppresses expression of hepatocyte growth factor/scatter factor receptor c-MET and reduces migration and invasiveness of breast cancer cells. Clin Cancer Res 2001;7:2555–62.
23. Kim SJ, Johnson M, Koterba K, Herynk MH, Uehara H, Gallick GE. Reduced c-Met expression by an adenovirus expressing a c-Met ribozyme inhibits tumorigenic growth and lymph node metastases of PC3-4 prostate tumor cells in an orthotopic nude mouse model. Clin Cancer Res 2003;9:5161–70.
24. Michieli P, Mazzone M, Basilico C, et al. Targeting the tumor and its microenvironment by a dual-function decoy Met receptor. Cancer Cell 2004;6:61–73.
25. Date K, Matsumoto K, Kuba K, Shimura H, Tanaka M, Nakamura T. Inhibition of tumor growth and invasion by a four-kringle antagonist (HGF/NK4) for hepatocyte growth factor. Oncogene 1998;17: 3045–54.
26. Tomioka D, Maehara N, Kuba K, et al. Inhibition of growth, invasion, and metastasis of human pancreatic carcinoma cells by NK4 in an orthotopic mouse model. Cancer Res 2001;61:7518–24.
27. Burgess T, Coxon A, Meyer S, et al. Fully human monoclonal antibodies to hepatocyte growth factor with therapeutic potential against hepatocyte growth factor/c-Met-dependent human tumors. Cancer Res 2006;66:1721–9.
28. Cao B, Su Y, Oskarsson M, et al. Neutralizing monoclonal antibodies to hepatocyte growth factor/scatter factor (HGF/SF) display antitumor activity in animal models. Proc Natl Acad Sci U S A 2001;98: 7443–8.
29. Webb CP, Hose CD, Koochekpour S, et al. The geldanamycins are potent inhibitors of the hepatocyte growth factor/scatter factor-met-urokinase plasminogen activator-plasmin proteolytic network. Cancer Res 2000;60:342–9.
30. Christensen JG, Burrows J, Salgia R. c-Met as a target for human cancer and characterization of inhibitors for therapeutic intervention. Cancer Lett 2005;225:1–26.
31. Morotti A, Mila S, Accornero P, Tagliabue E, Ponzetto C. K252a inhibits the oncogenic properties of Met, the HGF receptor. Oncogene 2002;21:4885–93.
32. Sattler M, Pride YB, Ma P, et al. A novel small molecule met inhibitor induces apoptosis in cells transformed by the oncogenic TPR-MET tyrosine kinase. Cancer Res 2003;63:5462–9.
33. Wang X, Le P, Liang C, et al. Potent and selective inhibitors of the Met [hepatocyte growth factor/scatter factor (HGF/SF) receptor] tyrosine kinase block HGF/SF-induced tumor cell growth and invasion. Mol Cancer Ther 2003;2:1085–92.
34. Al Awar RS, Ray JE, Hecker KA, et al. 1,7-Annulated indolocarbazoles as cyclin-dependent kinase inhibitors. Bioorg Med Chem Lett 2004;14:3217–20.
35. Hays JL, Watowich SJ. Oligomerization-induced modulation of TPR-MET tyrosine kinase activity. J Biol Chem 2003;278:27456–63.
36. Corso S, Comoglio PM, Giordano S. Cancer therapy: can the challenge be MET? Trends Mol Med 2005;11:284–92.
37. Underiner TL, Herbertz T, Miknyoczki SJ. Discovery of small molecule c-Met inhibitors: evolution and profiles of clinical candidates. Anticancer Agents Med Chem 2010;10:7–27.
38. Pan BS, Chan GK, Chenard M, et al. MK-2461, a novel multitargeted kinase inhibitor, preferentially inhibits the activated c-Met receptor. Cancer Res 2010;70:1524–33.
39. Jo M, Stolz DB, Esplen JE, Dorko K, Michalopoulos GK, Strom SC. Cross-talk between epidermal growth factor receptor and c-Met signal pathways in transformed cells. J Biol Chem 2000;275:8806–11.
40. Smolen GA, Sordella R, Muir B, et al. Amplification of MET may identify a subset of cancers with extreme sensitivity to the selective tyrosine kinase inhibitor PHA-665752. Proc Natl Acad Sci U S A 2006; 103:2316–21.
41. Mekhail T, Rich L, Rosen L. Final results: a dose escalation phase 1 study of ARQ 197, a selective c-Met inhibitor, in patients with metatstatic solid tumors. J Clin Oncol 2009;27:Abstract 3548.
42. Yap TA, Frentzas S, Tunariu N. Final results of a pharmacokinetic and pharmacodynamic phase I trial of ARQ 197 incorporating dynamic contrast-enhanced magnetic resonance imaging (DCE-MRI) studies investigating the anti-angiogenic activity of selective c-Met inhibition. J Clin Oncol 2009;27:Abstract 3523.
43. Laux I, Goldman J, Just R. Phase 1 dose escalation trial (ARQ 197-111) evaluating combination of selective c-Met inhibitor ARQ 197 and erlotinib. J Clin Oncol 2009;27:Abstract 3549.